Journal of Nuclear Science and Technology

ISSN: 0022-3131 (Print) 1881-1248 (Online) Journal homepage: http://www.tandfonline.com/loi/tnst20

Development of General-Purpose Particle and Heavy Ion Transport Monte Carlo Code

Hiroshi IWASE , Koji NIITA & Takashi NAKAMURA

To cite this article: Hiroshi IWASE , Koji NIITA & Takashi NAKAMURA (2002) Development of General-Purpose Particle and Heavy Ion Transport Monte Carlo Code, Journal of Nuclear Science and Technology, 39:11, 1142-1151, DOI: 10.1080/18811248.2002.9715305

To link to this article: https://doi.org/10.1080/18811248.2002.9715305

Published online: 07 Feb 2012.

Journal of NUCLEAR SCIENCE and TECHNOLOGY, Vol. 39, No. 11, p. 1142–1151 (November 2002)

Development of General-Purpose Particle and Heavy Ion Transport Monte Carlo Code

Hiroshi IWASE[1], Koji NIITA[2] and Takashi NAKAMURA[1,*]

[1]*Department of Quantum Science and Energy Engineering, Tohoku University, Aoba, Aramaki, Aoba-ku, Sendai 980-8579*
[2]*Research Organization for Information Science and Technology, 2-4, Shirakata, Tokai-mura, Naka-gun, Ibaraki 319-1106*

(Received May 7 2002 and accepted in revised form September 18, 2002)

The high-energy particle transport code NMTC/JAM, which has been developed at JAERI, was improved for the high-energy heavy ion transport calculation by incorporating the JQMD code, the SPAR code and the Shen formula. The new NMTC/JAM named PHITS (Particle and Heavy-Ion Transport code System) is the first general-purpose heavy ion transport Monte Carlo code over the incident energies from several MeV/nucleon to several GeV/nucleon.

KEYWORDS: heavy ions, transport calculation, NMTC/JAM, JQMD, GEM, PHITS, computer codes

I. Introduction

Recently, high-energy heavy ions have been used in various fields of nuclear physics, material science, and medical applications, especially cancer therapy, and several high energy heavy ion accelerator facilities are now operating or planned for construction. Radioactive beam facilities using the spallation products from intense heavy ion beams are also under construction for nuclear physics, nuclear chemistry and for applications. The high-energy heavy ion constituents of cosmic radiation must be considered in space utilization, such as the international space station project (ISS). The interactions and transport phenomena of heavy ions in a medium including the human body must be well understood to estimate the dose absorbed by the patients during cancer treatment, to estimate the exposure of astronauts and scientists in space and to design the shielding of accelerator facilities. There existed hitherto only one heavy-ion transport code, HZTRAN,[1)] developed by NASA (National Aeronautics and Space Administration), but this code is a one-dimensional discrete ordinates calculation code only.

Recently Iwase *et al.* have developed the three-dimensional Monte Carlo code, HETC-CYRIC,[2)] for heavy ion transport calculation. The HETC-CYRIC code was programmed by incorporating a newly-developed Heavy Ion transport calculation Routine (HIR) into the HETC-3STEP[3)] which is the hadron transport Monte Carlo calculation code. The heavy ion transport routine HIR computes the production and the transport of fragments and residual nuclei (spallation products) through a chain of incident heavy ion reactions in a medium, and this routine combines the HIC code[4)] to simulate the nucleus-nucleus collisions and the SPAR code[5)] to estimate the projectile energy degradation in a medium, incorporating the calculation of incident heavy ion attenuation in a medium using the Shen formula.[6)]

The HETC-CYRIC code gives good agreement with the experimental data for neutron production yields from thick targets. But the HETC-CYRIC code had been developed mainly to calculate neutron yields from thick targets bombarded by high energy heavy ions, and only information on neutrons, protons, and pions can then be outputted in the HETC-CYRIC code. For wide application to the high energy heavy ion studies it is very important to evaluate the energy spectra and the energy deposition of all fragment particles and the spatial distribution of residual nuclei (spallation products) produced by high energy heavy ions.

We therefore aimed to develop a new heavy ion transport code, PHITS (Particle and Heavy Ion Transport code System), for general purpose calculations based on the NMTC/JAM code,[7)] which is widely used for the hadron transport calculation. In the PHITS code, the HIC code, which is used in the HETC-CYRIC code, was revised into the JQMD[8)] code for heavy ion nuclear reaction simulation. This is because the JQMD is based on more modern nucleus-nucleus reaction model QMD, while on the other hand the HIC is based on more traditional intranuclear-cascade-evaporation model.

II. NMTC/JAM Code

The high-energy particle transport code NMTC/JAM is an upgraded version of the NMTC/JAERI97[9)] code. The applicable energy range of NMTC/JAM is extended to 200 GeV for nucleons and mesons by introducing the high energy nucleon-nucleus reaction code JAM[10)] for the intranuclear cascade calculation. The extension of the applicable energy range for the nucleon-nucleus inelastic, elastic and differential elastic cross sections is achieved by employing new systematics. The Coulomb diffusion for charged particles has been implemented in the transport calculation, as well as, the particle transport in a magnetic field. Concerning the evaporation and fission processes, NMTC/JAM includes a new code, GEM[11)] developed by Furihata, using the Generalized Evaporation Model (GEM) based on the Weisskopf-Ewing model. In the GEM, 66 ejectiles up to Mg, not only in their ground states but also in their excited states, are taken into account. The GEM code calculates the final yields of light nuclei resulting from the de-excitation of residual nuclei with good accuracy.

The NMTC/JAM code incorporates various tally functions and the format of input and output data has been improved in a user-friendly manner. Both the CG geometry system, which

*Corresponding author, Tel.&Fax. +81-22-217-7910,
E-mail: nakamura@cyric.tohoku.ac.jp

is used widely by the HETC, NMTC, LAHET, and the GG geometry system, which is used by the MCNP code system, are available using the same description for all geometries as in the PHITS geometry input. The source types of cylinder (including the circle and pencil beam), rectangular (rectangle), Gaussian, generic parabola, sphere (spherical shell), file reading, and one user definition type, are supported for any energy distribution in the NMTC/JAM code. The importance and the forced collision for any region can be set.

Figure 1 shows the double-differential cross sections of neutrons produced from p (3 GeV) on ^{208}Pb cited from Ref. 7) as an example. The results of JAM reproduce the neutron yields in the entire energy range from the beam energy down to 1 MeV rather well.

Figure 2 shows the calculated double differential cross sections of neutron emission from 800-MeV proton-induced Pb reactions compared with the LAHET[12] results and the measured data cited from Ref. 10). The intranuclear cascade model, INC, developed by Bertini was used to obtain the information of the excited nuclei, which is the input in the GEM calculation. Since the INC model is also used in the LAHET calculation, the only difference between GEM and LAHET is in the calculation of the evaporation process. In Fig. 2 the LAHET results overestimate the experimental data in the low energy region, on the other hand, the GEM results agree very well with the measured data. It is clear that the GEM model shows an improvement on LAHET in the evaporation calculation.

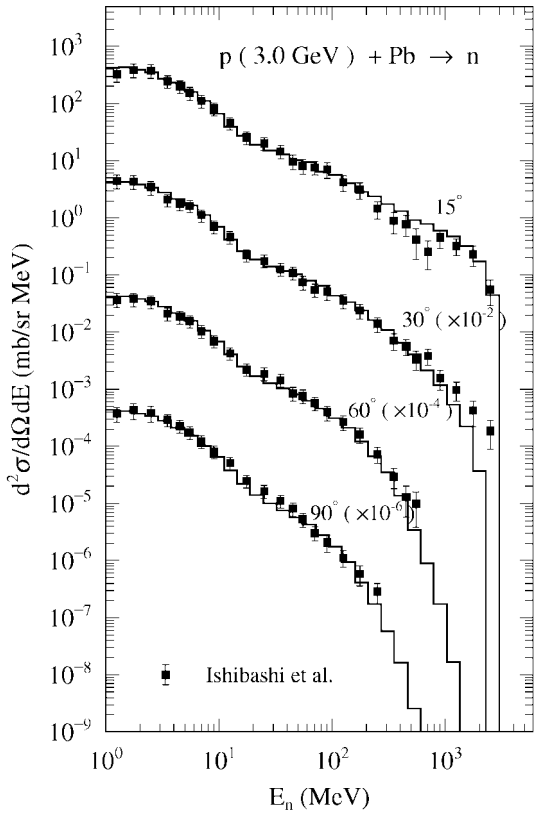

Fig. 1 Double-differential cross section of neutrons produced by 3 GeV proton on ^{208}Pb target calculated by the NMTC/JAM code cited from Ref. 7)

III. Heavy Ion Transport Calculation

The NMTC/JAM code cannot calculate the transport of composite particles, *i.e.* deuteron, triton, alpha particle and heavy ions, in a medium, so we incorporated the heavy ion transport calculation into the NMTC/JAM code.

1. Additional Codes

For the heavy ion transport calculation, Shen's formula, the SPAR code, and the JQMD[8] code are included in the NMTC/JAM code. The heavy ion transport calculation method in the PHITS code is schematically shown in **Fig. 3**.

(1) Shen's Formula

The Shen formula[6] is used to calculate the heavy ion total reaction cross sections described by

$$\sigma_t = 10\pi R^2 \left(1 - \frac{B}{E_{c.m.}}\right) \text{(mb)}, \tag{1}$$

where

$$B = \frac{1.44 Z_t Z_p}{r} - b\frac{R_t R_p}{R_t + R_p} \text{ (MeV)}$$

$$R = r_0 \left[A_t^{1/3} + A_p^{1/3} + 1.85\frac{A_t^{1/3} A_p^{1/3}}{A_t^{1/3} + A_p^{1/3}} - C'(E) \right] + \alpha \frac{(A_t - 2Z_t)Z_p}{A_t A_p} + \beta E_{c.m.}^{-1/3} \frac{A_t^{1/3} A_p^{1/3}}{A_t^{1/3} + A_p^{1/3}} \text{ (fm)}$$

$$r = R_t + R_p + 3.2 \text{ (fm)}$$

$$b = 1 \text{ (MeV/fm)}$$

$$R_x = 1.12 A_x^{1/3} - 0.94 A_x^{-1/3} \text{ (fm)}$$

$$(x = t: \text{ Target or } p: \text{ Projectile})$$

$$\alpha = 1 \text{ (fm)}$$

$$\beta = 0.176 \text{ (MeV}^{1/3}\text{)}$$

$$r_0 = 1.1 \text{ (fm)}$$

$C'(E)$: Transparency coefficient

$E_{c.m.}$: Projectile energy in the center of mass system (MeV)

in which

Z_t and Z_p are the atomic numbers of the target and the projectile,

A_t and A_p are the mass numbers of the target and the projectile,

R_t and R_p are the radii of the target and the projectile, respectively.

(2) SPAR Code

The SPAR code[5] is widely used to calculate the stopping powers and ranges for muons, pions, protons, and heavy ions at energies from zero to several hundreds GeV. **Figure 4** gives the calculated ranges of proton, helium, and oxygen ions in water cited from Ref. 5). Some differences are found in the low energy region below 1 MeV for proton and helium between calculation and experiment, but this discrepancy has little effect on the calculations because the PHITS transport code is mainly concerned with energies higher than several

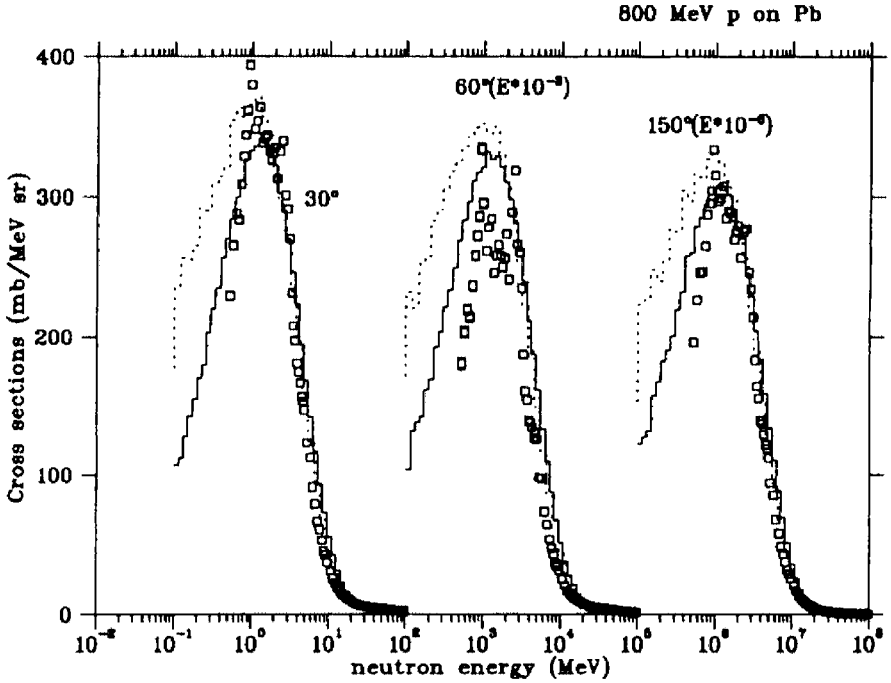

Fig. 2 Double differential cross sections of neutron emission from 800 MeV proton induced Pb reactions cited from Ref. 11)

The squares are experimental data, the solid lines are the INC/GEM results, and the dashed lines are the LAHET results.

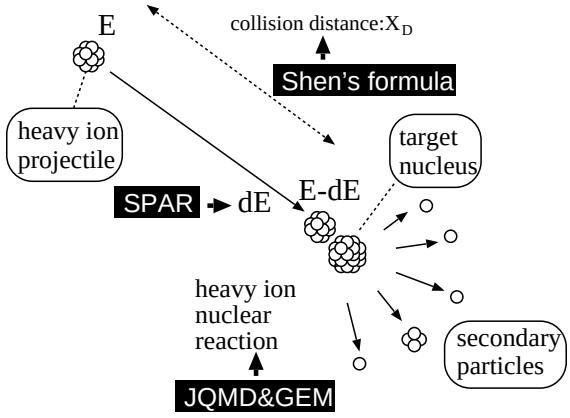

Fig. 3 Conceptual diagram of heavy ion transport calculation in the PHITS code

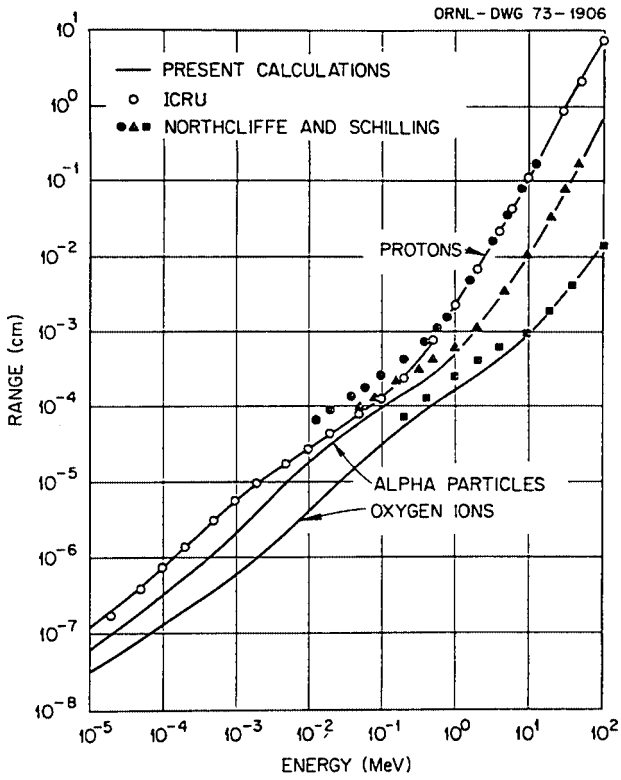

Fig. 4 Calculated ranges of proton, helium, and oxygen in water compared with the ICRU and measured data cited from Ref. 5)

MeV. Above 1 MeV energy both data and calculation of ranges agree well for all projectiles.

(3) JQMD Code

The JQMD (JAERI Quantum Molecular Dynamics) code,[8] which was developed by Niita *et al.* based on the QMD model, has been widely used to analyze various aspects of heavy ion reactions as well as of nucleon-induced reactions.[13] In the QMD model, the nucleus is described as a self-binding system of nucleons, which are interacting with each other through the effective interactions in the framework of molecular dynamics. One can estimate the yields of emitted light particles, fragments and of excited residual nuclei resulting from the heavy-ion collision.

The JQMD code has been included in the NMTC/JAM code only for nucleon-nucleus reaction and the JQMD routine was revised here in this study to be able to treat the nucleus-nucleus reaction in the PHITS code. We first show three ex-

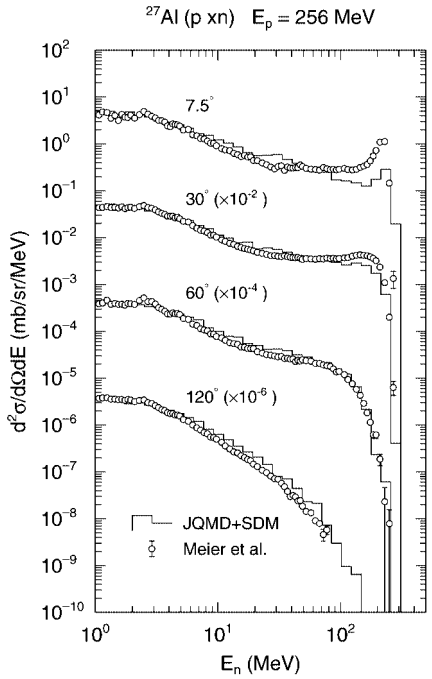

Fig. 5 JQMD calculation of the neutron double-differential cross section for 256 MeV proton on Al target cited from Ref. 8)

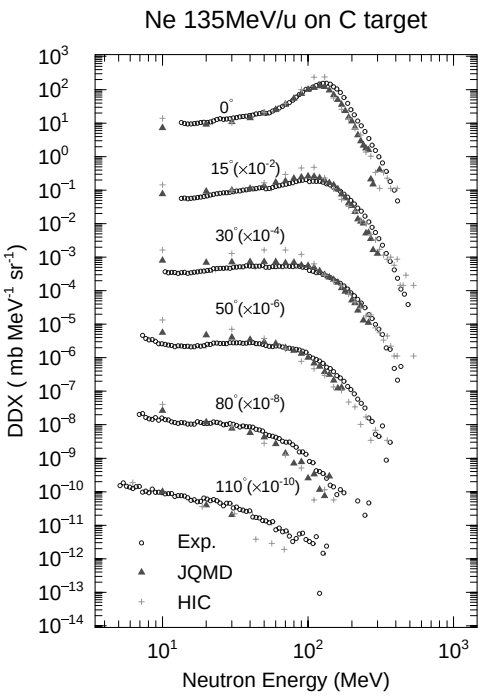

Fig. 6 JQMD calculation of the neutron double-differential cross section for 135 MeV Ne on C target compared with the HIC calculation and experimental data cited from Ref. 14)

amples of JQMD calculations for one nucleon-induced reaction and for two nucleus-induced reactions. **Figure 5** shows the double-differential cross sections of neutron production for 256 MeV proton on Al target calculated by the JQMD code compared with the data cited from Ref. 14). The JQMD results agree well with the measured data, with the possible except for the high energy peak at 7.5°. **Figure 6** shows the double-differential cross sections of neutron production for 135 MeV/nucleon Ne ions on C target calculated by the JQMD code compared with the data and the HIC calculation cited from Ref. 14). Above 135 MeV, which is the incident energy per nucleon of carbon projectile, both JQMD and HIC results underestimate the experimental data by a factor of two to three. Below 135 MeV down to 20 MeV the JQMD results agree rather well but tend to overestimate the data below 20 MeV by a factor of two. The JQMD results agree better with the measured spectra than the HIC results which overestimate in some cases by a factor three.

The double-differential cross sections data for 135 MeV/nucleon C ions on Cu target are shown in **Fig. 7**. JQMD calculation underestimates the measured data at the peak around 135 MeV at 0°, while HIC overestimates the peak. Above 135 MeV both the JQMD and the HIC underestimate the experimental data at forward angles from 0° to 50°. Nevertheless the JQMD results agree well with the data from 20 MeV to 100 MeV but below 20 MeV the JQMD code overestimates the data by a factor three. The HIC code gives larger values below 100 MeV at forward angles from 15° to 50° than the JQMD code. The broad peaks around 100 MeV at 80° and 110° in the HIC results are in disagreement with the data and these peaks are due to evaporation neutrons from the projectile in the HIC calculation. Compared with the proton-induced double-differential cross sections calculation,

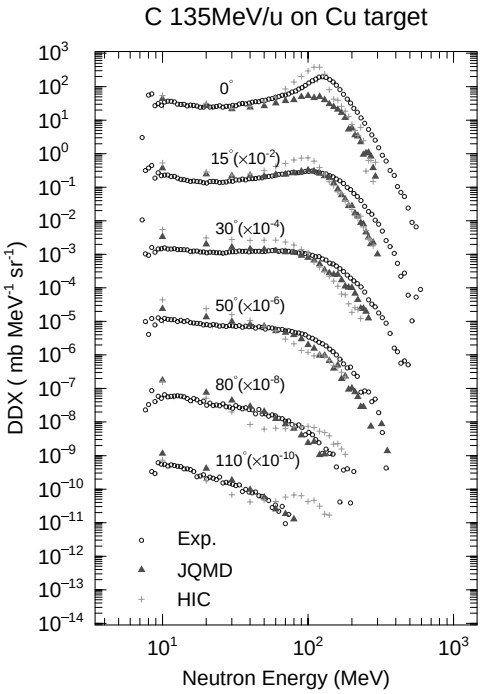

Fig. 7 JQMD calculation of the neutron double-differential cross section for 135 MeV C on Cu target compared with the HIC calculation and experimental data cited from Ref. 14)

the JQMD code tends to underestimate the data at 0° for the heavy-ion induced double-differential cross sections calculation.

From these comparisons, we confirmed that the JQMD code gives generally better agreement with the data than the HIC code.

2. Procedure of the Heavy Ion Transport Calculation

The distance X_D at which a heavy ion projectile travels before colliding with a target nucleus in a medium is taken randomly as follows:

$$X_D = \frac{\ln(r_n)}{\Sigma_t}, \tag{2}$$

where Σ_t is the total cross section of a projectile in a medium, which is calculated by Shen's formula Eq. (1), and r_n is a uniform random number.

The range X_R of a projectile in a medium can be calculated by the SPAR code. It is then decided whether a projectile collides or stops by comparing X_D and X_R. If $X_D < X_R$, a projectile collides with a target nucleus after the distance X_D by losing its energy continuously by neglecting straggling. This energy loss can be calculated by the SPAR code. If $X_D > X_R$, a projectile loses its energy completely without collision in a medium, and the transport of this projectile is not traced furthermore. The total cross sections change before and after collision due to energy degradation through the charged particle transport in a medium. This effect has already been considered in the NMTC/JAM code, which is incorporated in the PHITS code. When the collision point is determined, the heavy ion reaction calculations are treated by the JQMD code and the GEM code is used to calculate the evaporation from the excited nuclei after the JQMD calculation. After the heavy ion nuclear reaction, secondary-produced heavy ions are transported in the same manner as in the primary projectile transport calculation. For neutrons, protons, and pions the transport calculations are performed by the NMTC/JAM routine. All particles produced remain in the calculation until their energies or weights reach cutoff values, or until they go beyond the boundary of the calculation geometry.

IV. Comparison of the PHITS Code with the Measured Data

1. Double Differential Cross Section of the Neutron Calculation

In order to check the accuracy of the PHITS code, we first calculated the double-differential neutron production cross sections and compared with the data measured by Iwata *et al.*[15] They measured secondary neutrons produced from a carbon target of 10 cm by 10 cm square and 1.80 g/cm^2 thickness bombarded by 290 MeV/nucleon carbon ions. In the calculations the target size was fixed to the size used in the experiments and ring type detectors for surface crossing estimation were used to calculate the secondary neutron spectra as shown in **Fig. 8**. **Figure 9** shows the calculated results by comparing with the experimental data. This experiment uses a moderately thick target, which must be considered and the projectile energy loss of 10% corresponds to the projectile energy extending from 290 MeV/nucleon to 260 MeV/nucleon in the target. The energy width produces a broad peak in the forward direction in the neutron spectrum and this effect can be calculated in the PHITS code. In Fig. 9, the neutron energy spread in the high energy peak around 250 MeV/nucleon at 5° and 10° calculated with the PHITS code agrees well with the measured spectra. In the energy region below 100 MeV

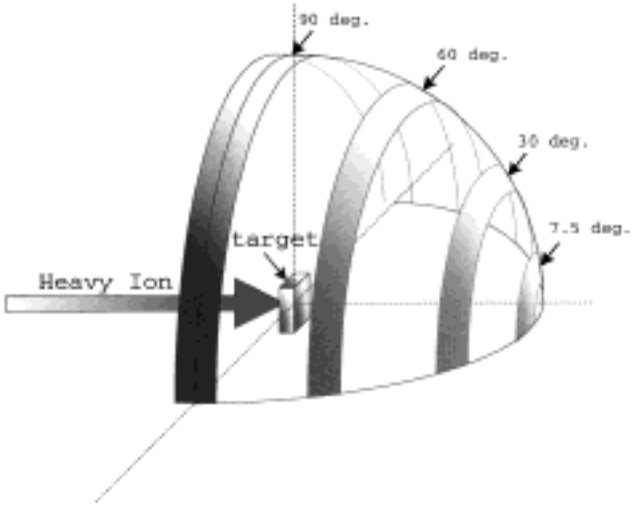

Fig. 8 Geometry of the calculation for the secondary neutron counting

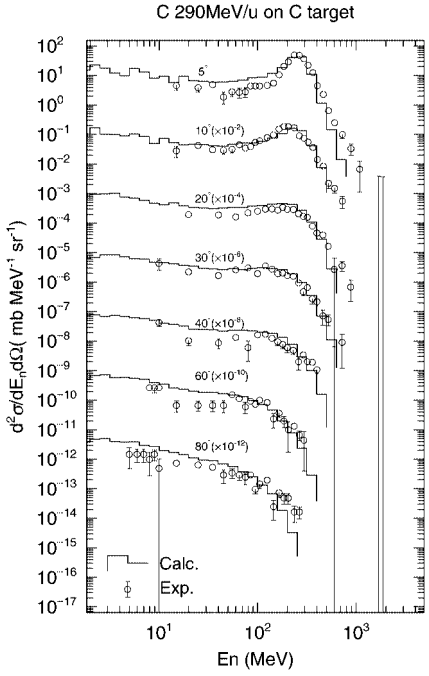

Fig. 9 Comparison of the neutron double-differential cross section calculated with the PHITS code and the measured data for 290 MeV/nucleon C ion on C target[15]

the calculation overestimates the measured data slightly, but above 100 MeV up to peak energy the calculated spectra agree well with the data at all angles. The PHITS results generally agree well with the experiments.

2. Thick Target Yield of the Neutron Calculation

We next investigated the accuracy of the PHITS code in the heavy ion transport calculation, by comparing with the data measured by Kurosawa *et al.*[16–19] They measured secondary neutrons produced from thick (stopping length) targets of C, Al, Cu, and Pb bombarded with various heavy ions from He to Xe. Incident energies ranged from 100 MeV/nucleon to

Table 1 Projectile type with its incident energy per nucleon and target thickness used in the experiment by Kurosawa *et al.*[16–19]

Projectile and energy (MeV)	Target and thickness (cm)			
He(100)	C (5.0)	Al (4.0)	Cu(1.5)	Pb(1.5)
He(180)	C(16.0)	Al(12.0)	Cu(4.5)	Pb(5.0)
C (100)	C (2.0)	Al (2.0)	Cu(0.5)	Pb(0.5)
C (180)	C (6.0)	Al (4.0)	Cu(1.5)	Pb(1.5)
C (400)	C(20.0)	Al(15.0)	Cu(5.5)	Pb(5.0)
Ne(100)	C (1.0)	Al (1.0)	Cu(0.5)	Pb(0.5)
Ne(180)	C (4.0)	Al (3.0)	Cu(1.0)	Pb(1.0)
Ne(400)	C(11.0)	Al (8.0)	Cu(3.0)	Pb(3.0)
Ar(400)	C (7.0)	Al (5.5)	Cu(2.0)	Pb(2.0)
Fe(400)	C (4.0)	Al (3.0)	Cu(1.5)	Pb(1.5)
Xe(400)	C (3.0)	Al (2.0)	Cu(1.0)	Pb(1.0)
Si (800)	C(23.0)		Cu(6.5)	

800 MeV/nucleon from the Heavy-Ion Medical Accelerator in Chiba (HIMAC) of the National Institute of Radiological Sciences (NIRS), Japan. **Table 1** shows the projectile types and energies, and the target thicknesses used in their experiment. Target sizes are 10 cm by 10 cm square.

In the calculations the target size was fixed to the size used in the experiments and the same ring type detector geometry as in Fig. 8 were used to calculate the secondary neutron spectra. We calculated the thick-target neutron energy spectra for all cases in Table 1. Generally speaking, the calculated results agree well with the measured data within a factor of three except for a few cases. The comparison between calculation and experiment is discussed in detail in the following cases.

In this comparison, the neutron transport through the target does not affect the secondary neutron spectra because the target size in this experiment is too small to consider neutron interaction in the target. The calculational accuracy of the neutron production from heavy ion projectiles with degraded energies while transporting through the target can therefore be checked in this comparison, which predominantly reduces to the accuracy of the JQMD code.

According to Refs. 16)–19) by Kurosawa *et al.*, the statistical uncertainties of the experimental data vary from 2 to 5% at the low to medium energies (about 10–100 MeV) of the spectra and increase to about 30% at the highest energies. For the results of the PHITS code the statistical uncertainties are plotted in the figures. The number of calculation histories of the PHITS code were at least 50,000 for each calculation shown in Figs. 10 to 12. It took three hours in the case of 100 MeV/nucleon carbon projectile on the carbon target but it took several days for 400 MeV/nucleon iron ion on the lead target using the Sun 500 MHz UltraSPARC-IIe CPU. The computing times depend on the mass numbers of projectile and target.

Figure 10 shows examples of PHITS calculations compared with the data for the cases of 100 MeV/nucleon carbon ions on thick carbon, aluminum, copper, and lead targets. Around the broad high energy peak region in forward direction of 0° and 7.5°, the PHITS results underestimate the measured data within a factor of three. The discrepancy in the peak region in forward direction, especially at 0°, for all targets may be caused by the JQMD model. This could be due to a momentum-dependent effective interaction neglected in the model.[12] It was already seen in Figs. 6 and 7 that the JQMD calculation underestimated the experimental results at 0° for light projectiles. The PHITS results agree well with the data at angles from 15° to 90° for all targets except for the lead target. For the lead target good agreement is obtained at larger angles of 30° to 90°.

Figure 11 shows the calculations for 400 MeV/nucleon carbon ion projectiles on carbon, aluminum, copper, and lead targets. At this higher projectile energy, the JQMD results still underestimate the yield in the peak region at 0° for all targets similarly to the 100 MeV/nucleon carbon case, but the agreement with the experiment around the peak at 7.5° is better. Although the JQMD calculations underestimate the measured yield above the projectile energy per nucleon (400 MeV) for all targets the agreement between calculation and experiment becomes better at higher energy projectile of 400 MeV/nucleon than that of 100 MeV/nucleon. Discrepancies between calculation and experiment below about 3 MeV might be due to experimental uncertainties.

Figure 12 shows the thick target neutron yield spectra calculations for the 400 MeV/nucleon iron ion case. The PHITS code still underestimates the measured data at 0° but the discrepancy is smaller than in the 100 MeV/nucleon and 400 MeV/nucleon carbon cases. This comparison indicates that he JQMD code has good calculational accuracy for heavy mass nucleus-nucleus reactions. Although the yields are underestimated at 7.5° on carbon, aluminum, and copper targets, the PHITS results generally agree quite well with the experimental data at higher energies and for heavier projectiles.

For the other cases listed in Table 1 calculations are not shown but results agree with the measured data as well as in Figs. 10 to 12. The calculations agree particularly well at large angles, from 30° to 90°, which indicates that the JQMD+GEM model offers good accuracy in the evaporation stages of the calculation of heavy ion nuclear reactions.

V. Conclusions

We improved the high-energy hadron transport code NMTC/JAM for use with high-energy heavy ion transport calculations by incorporating the JQMD code, the SPAR code and Shen's formula, and thus developed the PHITS code. The PHITS code is one of the first general-purpose heavy ion transport Monte Carlo codes applicable to energies from several MeV/nucleon to several GeV/nucleon.

It is confirmed from the comparison with measurements that the PHITS code provides good results on the angular distributions of secondary neutron energy spectra produced from thick carbon, aluminum, copper, and lead targets bombarded by 100 MeV/nucleon carbon, 400 MeV/nucleon carbon, and 400 MeV/nucleon iron ions.

Further investigations have begun to check the accuracy of the heavy ion transport calculation PHITS code, particularly for secondary charged particle emission and for heavy residual nuclei created in the heavy ion reactions. We conclude that this code can be applied to evaluate the neutron produc-

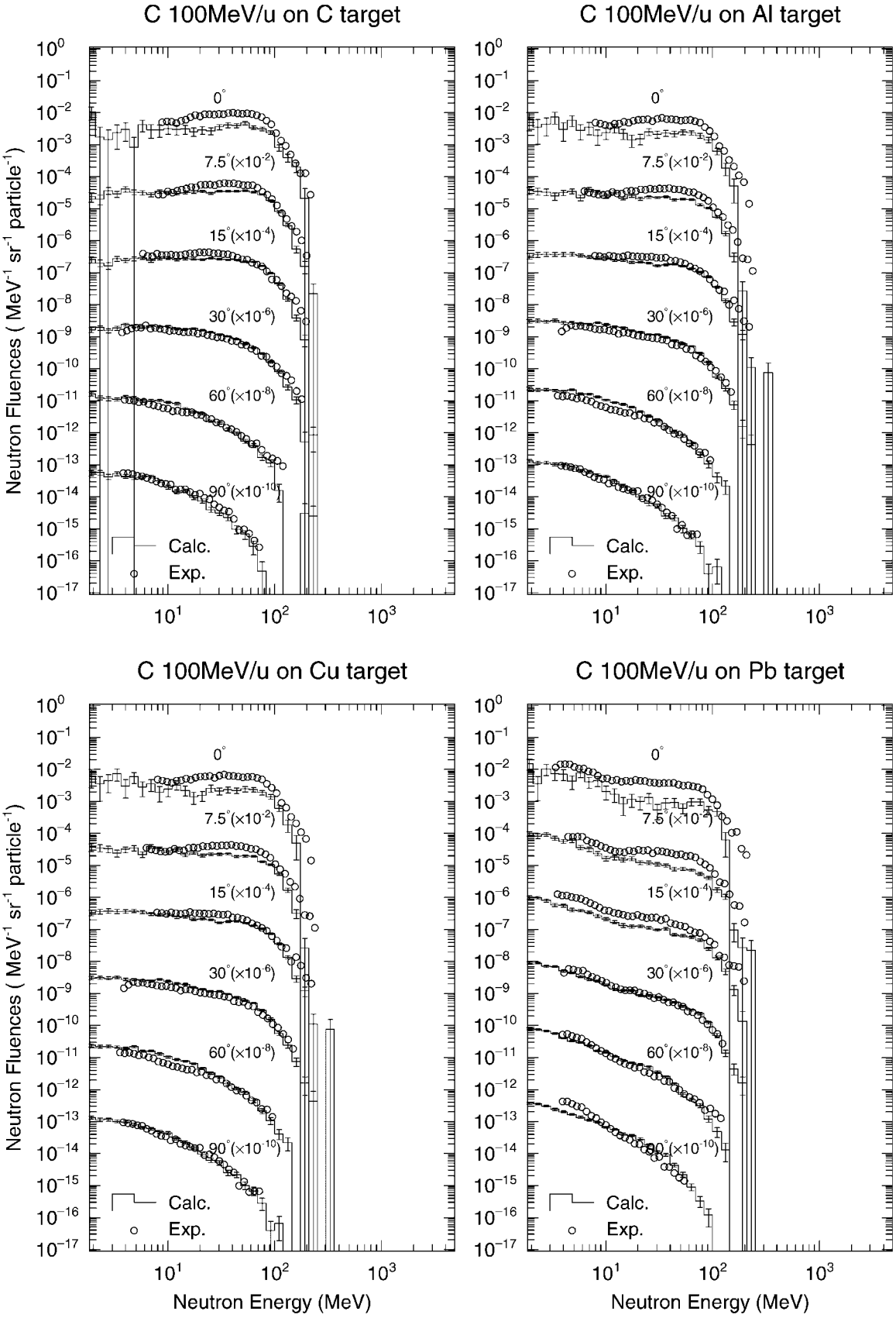

Fig. 10 Comparison of the neutron spectra calculated with the PHITS code and the measured data for 100 MeV/nucleon C ion on C, Al, Cu, and Pb targets[16)]

tion induced by the high energy heavy ion and this code will be used for wide range of heavy ion studies.

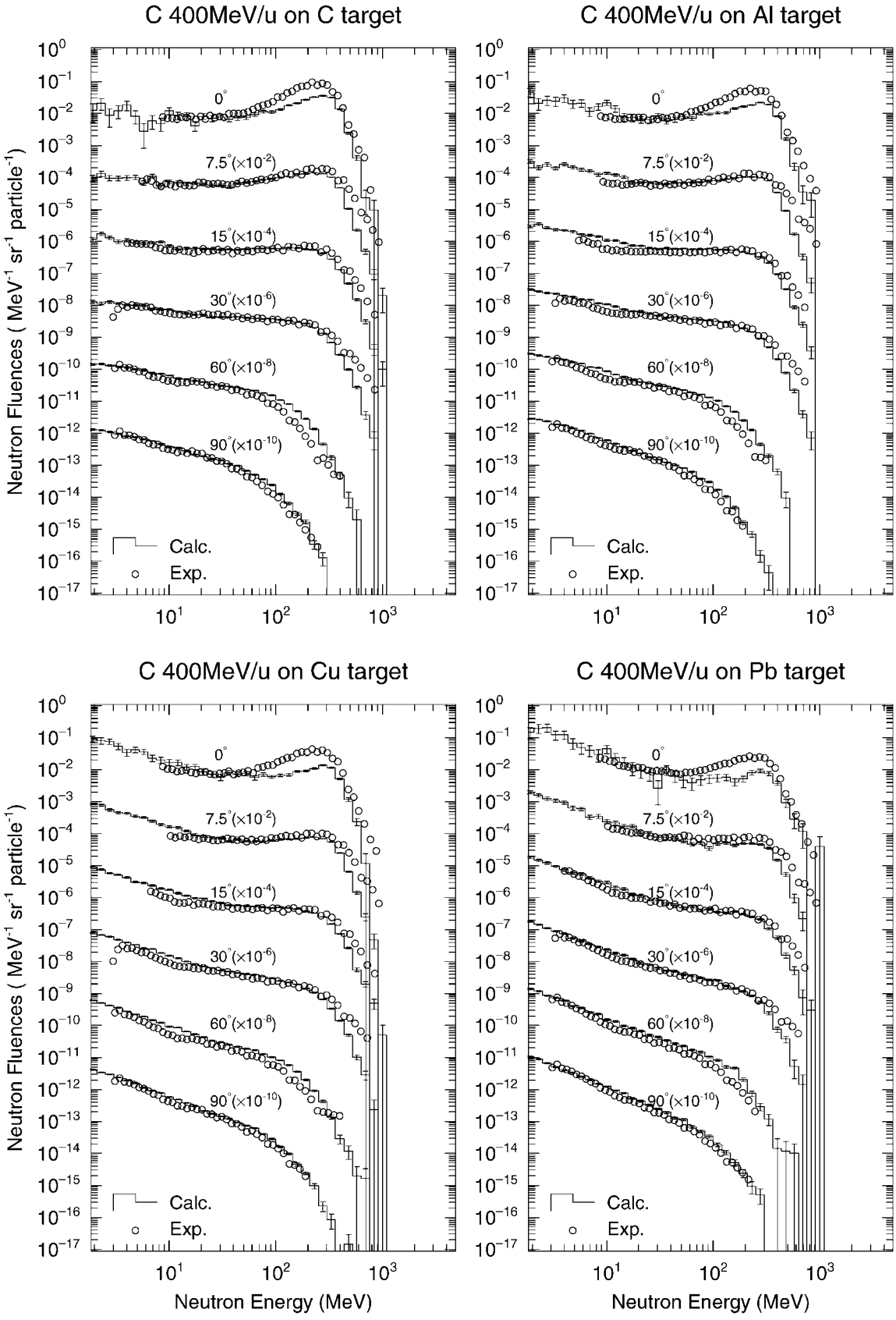

Fig. 11 Comparison of the neutron spectra calculated with the PHITS code and the measured data for 400 MeV/nucleon C ion on C, Al, Cu, and Pb targets[16)]

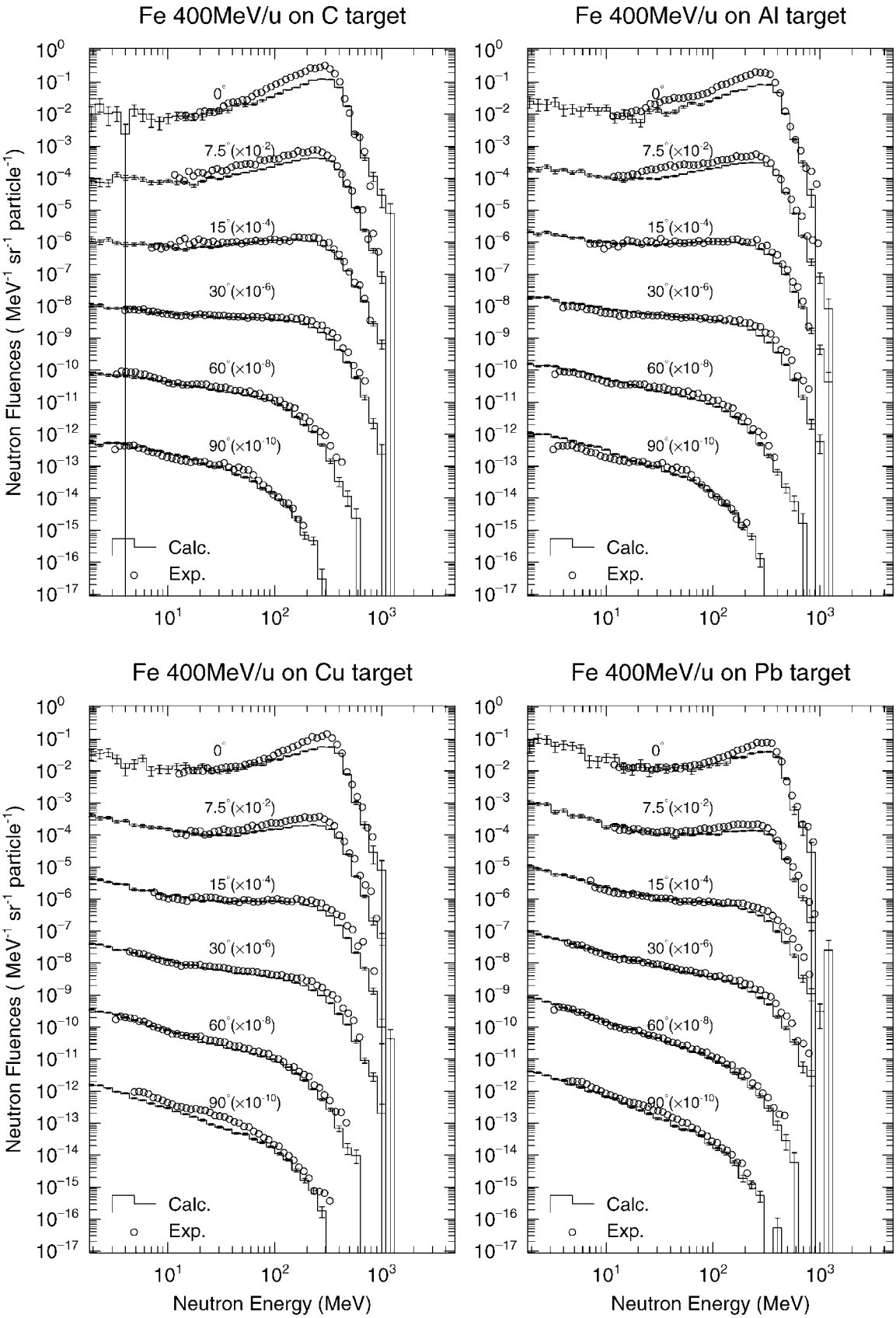

Fig. 12 Comparison of the neutron spectra calculated with the PHITS code and the measured data for 400 MeV/nucleon Fe ion on C, Al, Cu, and Pb targets[19)]

Acknowledgments

We wish to express our gratitude to Dr. Y. Yamaguchi and Dr. Y. Ikeda for supporting our work at Japan Atomic Energy Research Institute. We also would like to thank Dr. E. Kim, Dr. M. Harada, and Dr. S. Meigo for their contributions.

References

1) J. W. Wilson, S. Y. Chun, F. F. Badavi, L. W. Townsend, S. L. Lamkin, NASA TP-3146, National Aeronautics and Space Administration, (1991).
2) H. Iwase, T. Kurosawa, T. Nakamura, N. Yoshizawa, J. Funabiki, *Nucl. Instrum. Methods*, **B183**, 374 (2001).
3) N. Yoshizawa, K. Ishibashi, H. Takada, *J. Nucl. Sci. Technol.*, **32**, 601 (1995).
4) H. W. Bertini, T. A. Gabriel, T. T. Santoro, *et al.*, ORNL-TM-4134, Oak Ridge National Laboratory, (1974).
5) T. W. Armstrong, K. C. Chandler, ORNL-4869, Oak Ridge National Laboratory, (1973).
6) S. Wen-quinf, W. Bing, F. Jun, Z. Wen-logn, Z. Yong-tai, F. En-pu, *Nucl. Phys.*, **A491**, 130 (1989).
7) K. Niita, H. Takada, S. Meigo, Y. Ikeda, *Nucl. Instrum. Methods*, **B184**, 406 (2001); K. Niita, S. Meigo, H. Takada, Y. Ikeda, JAERI-Data/Code, 2001-007, Japan Atomic Energy Research Institute, (2001).
8) K. Niita, S. Chiba, T. Maruyama, H. Takada, T. Fukahori, Y. Nakahara, A. Iwamoto, *Phys. Rev.*, **C52**, 2620 (1995).
9) H. Takada, N. Yoshizawa, K. Kosaka, K. Ishibashi, JAERI-Data/Code, 98-005, Japan Atomic Energy Research Institute, (1998).
10) Y. Nara, N. Otuka, A. Ohnishi, K. Niita, S. Chiba, *Phys. Rev.*, **C61**, 024901 (1999).
11) S. Furihata, *Nucl. Instrum. Methods*, **B171**, 251 (2000).
12) R. E. Prael, H. Lichtenstein, LA-UR-89-3014, Los Alamos National Laboratory, (1989).
13) S. Chiba, O. Iwamoto, T. Fukahori, K. Niita, T. Maruyama, T. Maruyama, A. Iwamoto, *Phys. Rev.*, **C54**, 285 (1996); M. B. Chadwick, S. Chiba, K. Niita, T. Maruyama, A. Iwamoto, *Phys. Rev.*, **C52**, 2800 (1995); S. Chiba, M. B. Chadwick, K. Niita, T. Maruyama, T. Maruyama, A. Iwamoto, *Phys. Rev.*, **C53**, 1824 (1996); S. Chiba, K. Niita, O. Iwamoto, *Phys. Rev.*, **C54**, 3302 (1996).
14) H. Sato, T. Kurosawa, H. Iwase, T. Nakamura, U. Uwamino, N. Nakao, *Phys. Rev.*, **C64**, 34607 (2001).
15) Y. Iwata, L. Heilbronn, H. Sato, K. Niita, *et al.*, *Phys. Rev.*, **C64**, 054609 (2001).
16) T. Kurosawa, N. Nakao, T. Nakamura, U. Uwamino, T. Shibata, N. Nakanichi, A. Fukumura, K. Murakami, *Nucl. Sci. Eng.*, **132**, 30 (1999).
17) T. Kurosawa, N. Nakao, T. Nakamura, Y. Uwamino, T. Shibata, A. Fukumura, K. Murakami, *J. Nucl. Sci. Technol.*, **36**[1], 42 (1999).
18) T. Kurosawa, T. Nakamura, N. Nakao, T. Shibata, Y. Uwamino, A. Fukumura, *Nucl. Instrum. Methods*, **A430**, 400 (1999).
19) T. Kurosawa, N. Nakao, T. Nakamura, H. Iwase, H. Sato, Y. Uwanimo, A. Fukumura, *Phys. Rev.*, **C62**, 044615 (2000).